Aalto University
School of Science
Degree Programme in Computer Science and Engineering

Tiago Ferreira

Catch the dream Wave

Propagation of Cortical Slow Oscillation to the Striatum in anaesthetised mice

Master's Thesis
Espoo, July 31, 2014

Supervisor: Professor Juho Rousu
Professor Erik Aurell
Advisor: Ramon Reig PhD

Aalto University
School of Science
Degree Programme in Computer Science and Engineering

ABSTRACT OF
MASTER'S THESIS

Author: Tiago Ferreira

Title:
Catch the dream Wave Propagation of Cortical Slow Oscillation to the Striatum in anaesthetised mice

Date: July 31, 2014 **Pages:** 52

Major: Computational Systems Biology **Code:** T-61

Supervisor: Professor Juho Rousu
Professor Erik Aurell

Advisor: Ramon Reig PhD

Under anaesthesia or in deep sleep, different parts of the brain have a distinctive slow oscillatory activity, characterised by states of high membrane potential and intensive spiking activity, the Up-states; followed by hyper-polarisation and quiescence, the Down-states. This activity has been previously described *in vitro* and *in vivo* in the cortex and the striatum, across several species. Here, we look into it, during anaesthesia, in the mouse brain.

Using whole-cell patch-clamp recordings of cortical cells, it was possible to compare different signal processing methods used to extract the Up-and-Down states in extracellular recordings of the cortex. Our results show that the method based on the Multi-Unit Activity ($> 200Hz$) have better accuracy than High-Gamma Range ($20 - 100Hz$) or wavelet decomposition ($< 2Hz$ band).

After establishing the most robust method, this was used to compare the intracellular recordings of striatal cells to different parts of the cortex. The results obtained here support a functional connection between the dorsolateral striatal neurons and the ipsilateral barrel field. They also support a functional connection between dorsomedial striatal cells and the primary visual cortex.

The analysis of delay between recordings allowed to establish temporal relationships between the contralateral barrel field, the ipsilateral barrel field, and the dorsolateral striatum; and between the ipsilateral barrel field, the ipsilateral primary visual field and the dorsomedial striatum.

Keywords: Cortex, Striatum, anaesthesia, slow oscillation, spontaneous activity, ketamine, in vivo, up states, wavelet, MUA, high-gamma range, MSNs

Language: English

Acknowledgements

I wish to thank everyone. My family who has always supported me, my friends who make life so sweet, and my peers who help me move forward.

Espoo, July 31, 2014

Tiago Ferreira

Abbreviations and Acronyms

Acronym	Explanation
In vitro	the electrophysiological recordings are carried on a brain slice that is preserved and maintained in artificial extracellular fluid.
In vivo	electrophysiological recordings are carried in a live animal.
Intracellular	electrophysiological recording of a single cell, where the electrical activity can be read directly from the soma.
Extracellular	electrophysiological recording that captures the activity of several cells surrounding the electrode. This activity represents the average behaviour of the population.
CoIn	Coincidence Index, measurement of how well two or more sequences of Up-and-Down states overlap. In this text, CoIn refers to the average CoIn, which is an average between the CoIn for the Up state and the CoIn for the Down state.
LFP	Local Field Potential, equivalent to Extracellular recording in this context.
HGR	High Gamma Range, neural oscillations with frequency components between 20-100Hz in the extracellular recordings. Here, we also use this acronym to refer to the Up-and-Down state classification method, based on this frequency range.

MUA	Multi Unit Activity, signal extracted from extracellular recording that contains the high frequency components ($>$ 200 Hz) of the signal. These can be seen as an estimate of the spiking activity near the electrode. Our definition is the same as [30][37].Here, we also use this acronym to refer to the Up-and-Down state classification method, based on this frequency range.
SSO	Sleep Slow Oscillations, is a neural oscillations in the frequency range of $< 1Hz$ ($0.8Hz$ for humans), found during deep sleep or anaesthesia. They are an important part of Slow-Wave Sleep (SWS), and are the basis of synchronisation for higher frequency components, such has sleep spindles and ripples[25]. They have an important functionality in memory formation.[8].
CTX	Cortex, the outer layer of the brain.
BFl	Ipsilateral barrel field, situated in the primary sensory cortex (S1). The term ipsilateral means that it is in the same hemisphere as the part that it is being related to. For example, the left barrel field is ipsilateral to the striatum in the left hemisphere.
BFr	Contralateral barrel field, situated in the primary sensory cortex (S1). The term contralateral means that it is in the opposite hemisphere as the part that it is being related to. For example, the right barrel field is contralateral to the striatum in the left hemisphere.
MSN	Medium Spiny Neurons, this type of neuron compromises most of the neurons in the striatum, and is so called due to a high prevalence of spines in the dendrites.
S1	Primary somatosensory cortex.
M1	Primary motor cortex.
V1	Primary visual cortex.
DLS	Dorsolateral striatum.
DMS	Dorsomedial striatum.
$\tau_{(X,Y)}$	Lag between X and Y, is the time delay from signal X to Y. If positive, it means X is delayed in relationship to Y. If negative, Y is delayed in relationship to X.
C57BL6	C57 black 6, is a strain of laboratory mice. It is the most widely used strain, due to its genetic uniformity.

Contents

Chapter 1

Introduction - What is the dream Wave?

When we think about sleep, the first thing that comes to mind is stillness, quietude, peace. In fact, if you could look at yourself sleeping, you would probably see a calm version of your daily self, just lying there, more relaxed than ever. Even though your body remains still, your brain does not.
As you fall asleep, your brain goes through different stages of sleep, in a cyclic manner. At first, you enter Non-rapid eye movement sleep (NREM), which is divided into three phases. After these three phases, your muscles are paralysed, but your eyes start a rapid and random series of movements, entering what is called a Rapid eye movement sleep (REM). This process repeats itself until you wake up. All these phases are characterised by different brain activity.[36]
It is during the REM sleep that we dream, but right before REM sleep we have the 3^{rd} stage of NREM sleep. In NREM stage 3 the brain undergoes what is defined as Slow-Wave-Sleep (SWS), a phase that is characterised mainly by the propagation os the Sleep Slow Oscillation (neural oscillation with a frequency $< 1Hz$), which synchronises the activity of two other neural oscillations: sleep spindles ($12 - 14Hz$) and sharp wave-ripples ($140 - 200Hz$)[29].
Why is this oscillation so important? Because it groups and synchronises different neural oscillations across the brain [25], giving rise to consolidation of memory. According to Diekelmann[8], during wakefulness the brain performs the retrieval of long-term memories or encodes new memories in the short-term memory. Once the individual falls asleep, the brain starts a process of consolidation of the new memories into the long-term memory through two different mechanisms. One is related to the synaptic consolidation of memories, and occurs during REM sleep; and the other is the active consoli-

dation of memories, which occurs during Slow-Wave-Sleep. During SWS, the most prominent feature is the sleep slow oscillation, which originates in the neocortex, and propagates through the brain. This wave has a frequency of $0.8Hz$ (in Humans) and is characterised by two different states. An Up-state, where cells depolarise (higher membrane potential) and spike in a manner similar to wakefulness; and a Down-state, where cells hyperpolarise (lower membrane potential) and there is little to no spiking activity. The two states are called Up-and-Down, due to the difference in membrane potential of the cells involved. From an intracellular perspective, the membrane potential fluctuates between two stable values.[28][48].

1.1 Problem statement

As we have just seen, the Sleep Slow Oscillation has an important role in the brain activity. It originates in the cortex and propagates to the thalamus[47] and hippocampus[8], but it also propagates to the basal ganglia, namely to the Striatum.[16]
The basal ganglia is a set of deep brain structures that are involved in motor, learning, planning and decision making functions. One such structure is the striatum, which is the input layer of the basal ganglia. It receives excitatory synaptic transmission from most of cortical areas and the thalamus. Motor and sensory information from different modalities converge in striatal neurons, such as tactile or visual stimulation. However, it is not clear how the striatum integrates the information to generate proper outputs.
One way to help us understand how different information is integrated across the striatum is to look at the spontaneous activity that emerges in the cortex during anaesthesia, and how it propagates to the striatum. In fact, the cortical input to the striatum is enough to drive the striatal cells to a depolarised state or even elicit spikes.[53]. This input is afferent from different parts of the cortex, with different functions. For that reason, we studied the influence of the primary motor cortex (M1), the primary sensory-motor cortex (S1) and the primary visual cortex (V1).
The spontaneous activity that comes with the Sleep Slow Oscillation is complex, so we focus here on determining the states of the recordings in order to understand what can be learned from them and how the wave is propagating. In order to do so, we establish a comparison between different methods[16][30][39] used to extract the Up-and-Down state of the oscillation.Once we have picked a suitable candidate, we study how the information flows across the cortex, and into the striatum. For that, we checked if the cells in different parts of the brain were in similar states or not (Coincidence),

and how delayed the Slow Oscillation was between them(Time delay).
Is the spontaneous activity enough to understand how the brain processes information? The information extracted from the Slow Oscillation was enough to detect functional and temporal relationships between different areas of the cortex and the striatum, similarly to what was determined using active stimulation of the different sensory modalities[35].

1.2 Brief overview

I hope this Introduction gave the reader a sense of what is to come, and what are the questions we tried to elucidate with this work.
The following chapter introduces the reader to some basic concepts of neuroscience, as to make it easier to understand the rest of this project.
The 3^{rd} chapter provides information on the technical methods used to perform the recordings. Even though the reader is advised to read this chapter, the rest of the thesis is self-contained. This chapter is a supplement to it, for those interested in the methods.
The 4^{th} chapter concerns the signal processing methods used to extracted the Up-and-Down state sequences from the Sleep slow oscillations.
The 5^{th} chapter concerns the implementation of signal processing and extraction of the Up-and-Down state. This chapter is not essential for understanding the thesis, but it does present some important considerations that had to be taken into account during the implementation and development of the project. Here, noise, short Up-and-Down states and other problems are discussed and their respective solutions are presented.
In chapter 6 the results are presented and discussed.
The last chapter, is a final discussion, where the main points of the project are re-visited, and some new research questions are proposed.

Chapter 2

Background - A sea of Knowledge

Before we dive into the problem of finding and characterising the slow-oscillation, it is good to know a little about what waters we are swimming in.

Coordinate system - When we think of the brain, and more specifically if we are to consider how a wave propagates through it, we need to have a common nomenclature to refer to different positions, and directions. For that reason, in neuroscience, like in other biological sciences, we use a coordinate system based on the morphology of living creatures.

Imagine you are walking in a park, and a friendly dog comes to play with you. As you look straight at it, the first thing you see is its head, and then the rest of the body up to the tail. You can say that the tail is in a posterior position, whereas the head is in an anterior position. You then pat him in the back, which is the dorsal area. It rolls over so you can scratch its belly, which is the ventral area. You proceed to pat him on the side, a lateral position. One could say that this gesture touched its heart, which, by the way, is in a medial position (in the middle). These terms can also be used in a relative manner, for example, your eyes are posterior to your nose, but anterior to your ears.

This same nomenclature is used to describe the brain positions in both humans and animals. Notice however, that since humans are bipedal, some of the axis can be a source of confusion. (see figure 2.1)

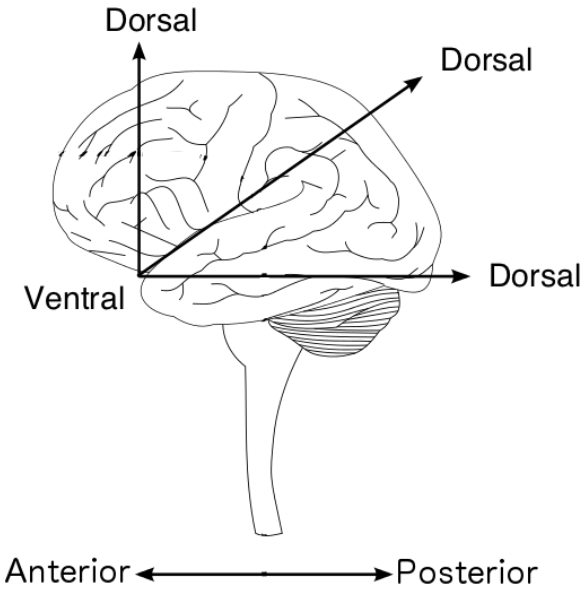

Figure 2.1: The bipedality of humans causes the ventral-dorsal axis to fold. Since humans stand in an upright position, with their necks bent to face forward, the ventral dorsal axis is not orthogonal to the anterior posterior axis. Image adapted from Wikimedia Commons, original image created by user Juoj8 and shared under the Creative Commons Attribution-Share Alike 3.0 Unported license.

2.1 The cortex - Where the wave begins

The slow sleep oscillation propagates in a anteroposterior direction[25], this means it will go from the front of the forehead to the back of the skull. If we could follow the slow sleep oscillation in the mouse brain, it would start in the anterior part of the frontal lobe and eventually reach its posterior part. Here, it would be in the primary motor cortex (M1) (see Figure 2.4), an area that processes motor information. The primary motor cortex is part of a larger network that processes motor information. This network is composed by the medial premotor cortex, the lateral premotor cortex and the primary motor cortex. Together they mediate conscious movement, i.e., planning and initiation of complex movement sequences. The primary motor cortex enervates several lower cortex areas, such as the brainstem or pons. These enervations allow for the activation of motor sequences. A closer look at

the functionality of the primary motor cortex, shows that there is a direct mapping between different areas of the primary cortex, and different parts of the body. (see figure 2.2) At a finer scale, this division is not so clear, as some areas overlap or activate organised movements rather than individual movements.

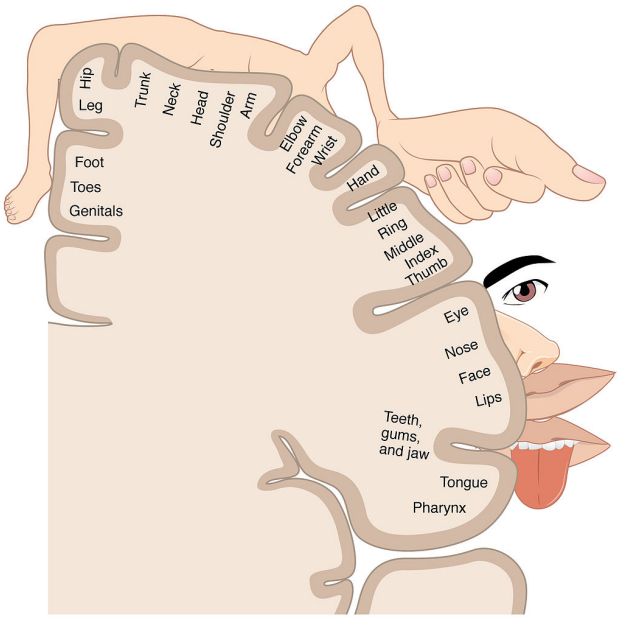

Figure 2.2: Spatial mapping of the body in humans. This picture represents the spatial mapping of the different parts of the body to the cortex near the central gyrus. This mapping is similar for the primary motor cortex and the primary sensory cortex. This figure is licensed by Rice University under a Creative Commons Attribution License (CC-BY 3.0), and is an Open Educational Resource.

From the primary motor cortex, the wave would then travel to the primary somatosensory cortex (S1) (see Figure 2.4). Similarly to M1, there is a spatial relationship between areas of S1 and different areas of the body, but unlike the motor cortex that processes motor activity, the somatosensory processes sensorial activity (examples of this activity are touch, pain or heat). In humans, big areas of S1 are dedicated to the face and the hands, due to their importance in capturing the world around us. In mice, part of this job is accomplished by the whiskers, which have their representation on the Barrel Field (BF). (see figure 2.3)

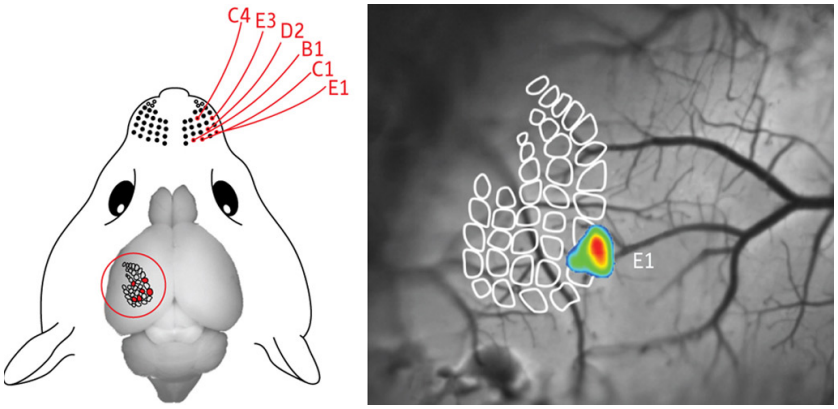

Figure 2.3: Spatial mapping of the mouse whiskers. This picture represents the spatial mapping of different whiskers to the barrel cortex in the primary somatosensory area of the mouse brain. Notice how the whisker E1 is clearly mapped in the barrel field. Reproduced, in part, from Ref.[3] © 2010 Walther Akemann et al.

After S1, the wave would keep on travelling until the most posterior part of the brain, the posterior pole of the occipital cortex. Here, it would reach the primary visual cortex (V1) (see Figure 2.4). V1 receives mainly visual input from the retina through the primary visual pathway. Here some of the main features of the image are extracted, such as movement, orientation, direction or speed. Similarly to M1 and S1, V1 is also a spatial map to parts of the body, but here they are specific to the eye. Different parts of the vision field are mapped into different parts of V1, with a structure similar to that found in the previous areas. What this means is that there are modular substructures, iterated across these regions, that involve thousands of neurons in repeating patterns. Each module responds to specific combinations of properties in visual stimuli. For example, in human V1, there are specific regions that react to specific combinations of rays and rings.[51] V1 then connects to higher order visual cortex, but also receives input from them.[19].
This was the anteroposterior trajectory of the sleep slow oscillation. Notice however that all cortical areas mentioned before connect to inner parts of the brain, namely to the striatum. (see Figure 2.4)

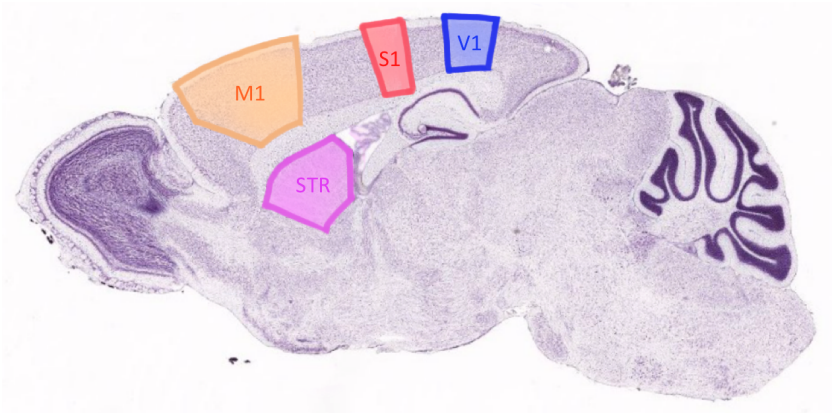

Figure 2.4: Brain areas where the sleep oscillation was analysed. The areas are as follow: primary motor area (M1) in orange; primary somatosensory area (S1) in red; primary visual area (V1) in blue; striatum (STR) in purple. Image adapted from Allen Mouse Brain Atlas.[1].

This means that the slow sleep oscillation could travel not only in a anteroposterior way, but also in a dorsal-ventral way. This is the case, as it has been shown that the sleep slow oscillation also travels from the cortex to the striatum[16]. The trajectory the wave travels in a dorsal-ventral direction is not so well understood, and is part of what is studied in this project. For that, we now focus on the inner brain, namely on the basal ganglia.
The basal ganglia is involved in learning, motor behaviour selection, emotion, among other cognitive functions. In fact, abnormalities in it are associated to cognitive and motor deficiencies such as Huntington's Disease or Parkinson's Disease [34].

2.2 The striatum - Riptide

One of the several components of the basal ganglia is the striatum. The striatum is a nuclei that lies deep within the cerebral hemispheres. In conjunction with the caudate, putamen, the globus pallidus, the substantia nigra and the subthalamic nucleus, it is responsible for motor action selection.
One way to study this structure, is to analyse the electrophysiological properties of different neurons. The electrophysiological properties of a neuron are its electrical response, namely its current and its voltage. These can be measured extracellularly or intracellularly. Extracellular recordings can be done with surface electrodes, that measure not the activity of a single neuron, but of a population of neurons close to the electrode. This type of measure-

ment is more noisy, but contains information regarding the local population, which can be used to extract spiking patterns (spike-sorting), and the extracellular potential caused by network responses of the whole population (local field potential). Intracellular recordings on the other hand, give us a reading of a single neuron, allowing to study not only the spiking activity, but also sub-threshold activity. This activity is representative of the way the single neuron operates. Since each individual neuron has its own connectivity patterns, this method does not provide a picture of the population or the functioning of the network. For the reasons mentioned earlier, extracellular recordings are more suited for the areas that provide excitation to the striatum, whereas intracellular recordings are more suited for studying the actual striatal neurons. Extracellular recordings are performed with surface electrodes, whereas intracellular require patch clamping. Both methods are invasive and require craniotomies.
The striatum receives afferents from both the thalamus and the cortex. The cortex input to the striatum is enough to drive the MSNs to a depolarised state or even to elicit action potentials.[53] The propagation of the cortical activity, namely visual and sensory motor activity, results in the integration and filtering of external information that could allow the selection of more appropriate behaviours.[32]. Another source of stimulation to the striatum is the motor cortex, and it is important to notice that any motor activity will induce noise in the measurements. Also, the motor cortex relays information from the sensory motor area to the striatum.[35] One way to reduce noise due to motor activity is to apply anaesthesia to the animal. Anaesthesia will not only suppress motor activity, but also reduce the activity of the thalamus[12]; making the anaesthesia state a good simplified model to study the influence of cortical activity on the striatum. More importantly, anaesthesia will induce slow oscillations, similar to those observed in Slow-Wave-Sleep.

Chapter 3

Environment - Getting ready

Before we can get on with studying the Sleep slow oscillation, we need to gather the data from experiments.
The used experimental protocol, as developed and performed by Ramon Reig, was the same as here[35].

3.1 Experimental Procedures

Ethical approval - All experiments were performed according to the guidelines of the Stockholm municipal committee for animal experiments.
Electrophysiological recordings - Adult C57BL6 mice of both sexes between 2-6 months of age were used to perform the experiments (n = 71). Anesthesia was induced by intraperitoneal injection of ketamine (75 mg/kg) and medetomidine (1 mg/kg) diluted in 0.9 % NaCl. A maintaining dose of ketamine (30 mg/kg i.m.) was administrated every 2 hours or after changes in the EEG or reflex responds to paw pinches. Animals were sacrificed after recordings by receiving an overdose of sodium pentobarbital (200 mg/kg I.P.). Tracheotomy was performed to increase mechanical stability during recordings by decreasing breathing related movements. Mice were placed in a stereotaxic device and air enriched with oxygen was delivered through a thin tube placed 1 cm from the tracheal cannula. Temperature was maintained between 36-37.5 ^{o}C using a feedback-controlled heating pad (FHC Inc.). Craniotomies were made at 5 sites for patch clamp and extracellular recordings: AP 0 mm from Bregma, L 2.5 mm (dorsomedial striatum); AP 0 mm from Bregma, L 3.75 mm (dorsolateral striatum); AP -1.5 mm, L 3.25 mm (S1); AP -3.5 mm, L 2.5 mm (V1); AP 1.5 mm, L 2 mm (M1). (following Paxinos and Franklin 2001)[31].

Intracellular recordings - Whole-cell recordings were obtained from dorsolateral striatum between 1854-2613 μm deep and in layer V of cortical barrel field between 617-863 μm from the pia, in a perpendicular penetration angle. Signals were amplified using MultiClamp 700B amplifier (Molecular Devices) and digitized at 20 KHz with a CED acquisition board and Spike 2 software (Cambridge Electronic Design). Patch pipettes were pulled with a Flaming/Brown micropipette puller P-87 (Sutter Instruments) and had an initial resistance of 5-12 $M\Omega$, with longer tips than the standard ones to minimize cortical damage. Pipettes were back-filled with intracellular solution containing the following (in mM): 125 K-gluconate, 10 KCl, 10 Na-Phosphocreatine, 10 HEPES, 4 ATP-Mg, 0.3 GTP-Na. A subset of experiments was performed with intracellular solution containing 105 K-gluconate, 30 KCl, 10 Na-Phosphocreatine, 10 HEPES, 4 ATP-Mg, 0.3 GTP-Na.
Extracellular recordings - Extracellular recordings were obtained using tungsten electrodes with impedances of 1-2 $M\Omega$. The electrodes were placed in infragranular layers in somatosensory (BF) and visual (V1) cortex with an angle between 15-25 degrees. Recordings were amplified using a Differential AC Amplifier model 1700 (A-M Systems) and digitized at 10 KHz with CED and Spike-2 simultaneously with the whole-cell recording.

Chapter 4

Signal processing - Looking at the waves

When we consider the Slow-wave-sleep, we want to take a better look at how the wave propagates. In order to do that, we extract the Up-and-Down states from the sleep slow oscillation. The easiest way to do so, is to look at intracellular recordings of cells, as they have a clear definition of the Up-and-Down states.

4.1 The Golden Standard: Intracellular recordings

Even though the slow oscillatory sleep activity had been previously described, it was not until 1993 that it was firstly quantified. It was back then, that Metherate and Ashe [28] used *in vivo* whole-cell recordings of neurons in the auditory cortex to characterise the variation of membrane potential of the slow oscillations.
Whereas in extracellular recordings the Up-and-Down state is characterised by several factors and its quantification is a complex problem, in intracellular recordings there is a clear Up-State characterised by a more depolarised cell potential and a higher firing rate, and the Down-state is characterised by a lower membrane potential and a smaller firing rate. This makes it possible to distinguish the Up-state from the Down solely based on the membrane potential.
Since then, intracellular recordings have been used in different types of cells [50][33], both *in vivo*[35][24] and *in vitro*[37][40][41]. Across these different experiments, when in the presence of Slow Oscillations, the distribution of membrane potential shows a bimodal distribution. For that reason, it is ad-

equate to use histogram-based methods for classification of the states. In these methods it is sufficient to determine a threshold value of membrane potential to distinguish between states. (see Figure 4.1)

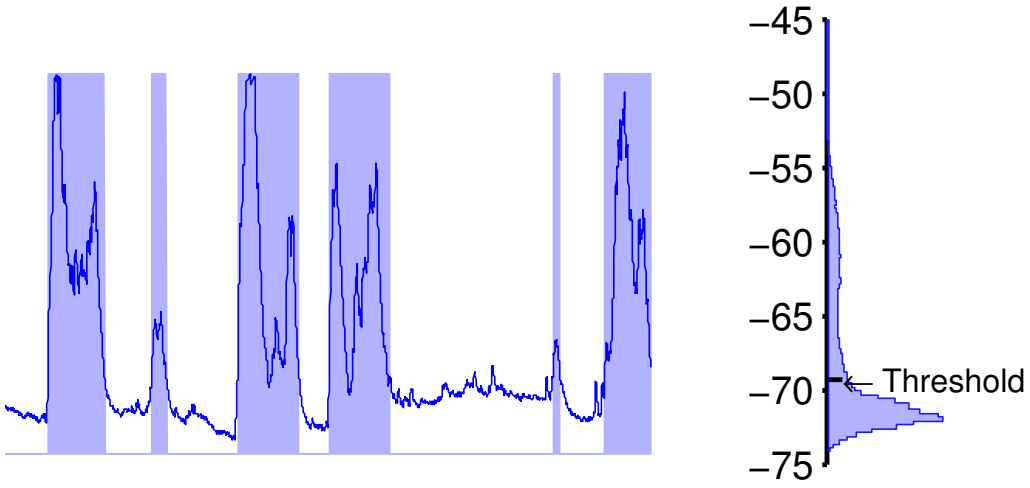

Figure 4.1: Classification of Up-and-Down-state. The Up-states are highlighted in light blue. On the right side, the distribution of the membrane potential and respective Threshold used for classification (mV).

We determine this threshold using an automated method, filter the original signal if in the presence of noise, and remove small states from the extracted state sequence (see Chapter 5 for details).
We determined, through comparison of mean membrane potential, and visual inspection, that the method produces a good classification of states. In the case of whole-cell patch-clamp recordings of cortical cells, their states can be used as a standard for comparison with the Up-and-Down states extracted from the extracellular recordings.[30]

4.2 Extracting Up-and-Down states from Extracellular recordings

The problem of extracting the Up-and-Down states from extracellular recordings is far more complex, and there are several approaches that have been suggested and used across different time periods. Whereas in the intracellular recording the membrane potential is a good indicator of the current

state, for extracellular recordings there are several components to take into account. Considering that the sleep slow oscillation has a frequency range of 0-2Hz, an earlier approach was to use wavelet decomposition to extract that frequency range, and evaluate the signal in regards to it. Since then, there has been a transition to new methods, based on contribution of high frequency fluctuations to the extracellular recording during active states.

4.2.1 The different methods

In this study, we focused on three different methods, based on different properties of the signal. The first, Wavelet decomposition, was chosen since it was a popular method in the early 2000's[2][6][11][18] and it allows to extract a frequency component which can be used not only for Up-and-Down state classification, but also for other purposes (e.g. instantaneous phase[16][15]). This method, however, has been contested earlier for giving contradictory results across different studies.[30] It is still in use nowadays for processing Electro Encephalogram (EEG)[14][22]. The second method, High-Gamma Range (HGR), is from 2007, and in the original paper[30], the authors use a measure of coincidence to evaluate the state classification, and fine tune their method to classify Up-and-Down states in their experimental conditions. We use the same process of evaluation in here to compare all three methods (see Chapter 6). This method was chosen due to its claimed efficiency. The last chosen method is based on Multi-Unit Activity (MUA), which has seen applications from predicting movement[46] to detection of Up-and-Down states[37]. We chose this method due to its previous applications, but also because it is based on spiking activity, which is one of the underlying processes on the generation of Up-states.[40]

Wavelet Decomposition - The Sleep Slow Oscillations main feature is its frequency $< 1Hz$. For that reason, if there was a way to capture just this behaviour out of the whole extracellular recording, then it would be possible to study it. That is the principle behind the wavelet transform. One can see the wavelet transform almost like a microscope[23], that allows to zoom in on the frequency components of a signal. Every time we zoom in, we see part of the picture in better detail, but we lose in field of view. Here, we can see part of the frequencies in higher detail, and lose the higher frequencies up to that point. At every "zoom" step, we filter and down-sample a signal. We keep doing this in an iterative manner until we are looking at the frequency band of interest. The other important factor, in this method, is the wavelet itself. There are different types of wavelets, and in wavelet decomposition, what we are doing is fitting our wavelet to the signal. This allows to expose the components of the signal that resemble the wavelet. You can imagine

it almost has using fluorescence microscopy. In fluorescence microscopy you only see the cells that reflect the radiation of your laser. In wavelet, you only see the features of the signal that better match your wavelet (that correlate with it).
We used the Matlab (The MathWorks, Inc., Natick, MA, USA) implementation of wavelet decomposition, with the discrete Meyer wavelet, to extract the $0-2Hz$ band. This band was then normalised to the interval [-1,1], and the zero-crossing point was chosen has the transition between state. The method is described in detail in the Signal analysis section of Kasanetz, 2006. [16]
For a formal introduction to the topic, refer to [52]. For a recent overview of the method, and its development into Sparse analysis, refer to Mallat, 2008 [21].
High Gamma frequency Range (HGR) - An extracellular recording done with a surface electrode, will capture the activity from several cells. In this sense, the Up-and-Down states of the extracellular recordings will be composed of the Up-and-Down states of several individual cells surrounding the electrode. By measuring the activity of one of these single cells, it is possible to determine its Up-and-Down states, which will coincide with the extracellular ones. If we then analyse the power spectra of the extracellular recording for Up-states and compare it to the power spectra of Down-states, we can find which frequencies have higher power in the Up-state. According to the literature, these have been determined to be the High-Gamma range $(20-100Hz)$ for NREM sleep[30]. (see Figure 4.2)

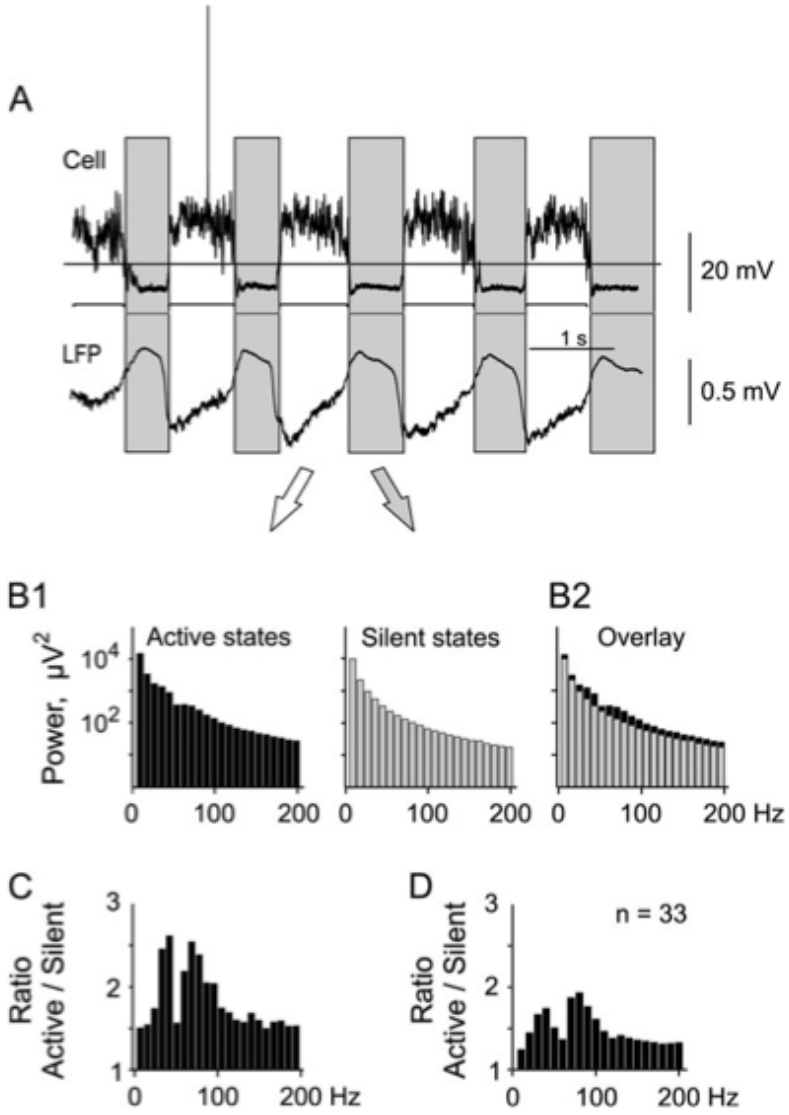

Figure 4.2: Comparison of power spectrum components in the extracellular recording during the active and silent states in cells. (A) Simultaneously recorded membrane potential and extracellular signals. Cell has clear active and silent states. The states were detected using a level shown as horizontal line. The detected active and silent states are shown with horizontal bars below the membrane potential trace. Large vertical gray bars mark periods of silent states in the cell. (B) Power spectra of the extracellular recordings during periods of the active and silent states in the cell (B1) and superposition of the 2 power spectra (B2). Power spectra are shown with bin width of 10 Hz. Ordinate scaling is logarithmic. Note that all components are smaller during the silent states but the difference is not uniform and depends on frequency. (C) Ratio of the corresponding power spectrum values during active and silent states, calculated for the data from (B). Note that the ratio is maximal in the range between 20 and 100 Hz. A trough around 60 Hz is due to the filtering used during the recording to reduce the contribution of the mains frequency. (D) Same as in (C), but averaged data for 33 cell-extracellular pairs. Note that the difference between active and silent states is largest at 20-100 Hz. Adapted from Mukovski (2007), by permission of Oxford University Press.

The signal can then be filtered on that specific band and further processed with the calculation of its standard deviation over a 5 ms window and smoothed with a 50 ms moving average filter.
This new signal displays a bimodal distribution similar to the one seen in intracellular recordings, and as such, it is only a matter of detecting a suitable threshold to separate the Up-state from the Down-state.
Multi Unit Activity (MUA) - Around the same time that the HGR method was developed, analysis of extracellular recordings was shifting from methods based on spike sorting[20][44][49][5], to methods that extract a measure of relative firing rate[46][9][37][39]. Given an extracellular recording, this can be filtered to extract two different signals. The first one is the Local Field Potential (LFP), and it represents the electric potential in the extracellular space around neurons.[7] This means that is captures the activity in the extracellular recordings, except for the spikes. The way to obtain it, is to extract the frequency range $1 - 100Hz$. The other signal is the Multi Unit Activity, and represents the spiking activity of the cells surrounding the electrode.
The MUA can be obtained by filtering the high-frequency range of the signal ($> 200Hz$), calculate its root mean square and smooth it in a similar fashion to the previous method. This normalised High-frequency component can be seen as a linear transformation of the instantaneous spiking activity surrounding the electrode tip.[26] Even though the problem os extracting single-spikes is complex and is usually performed with more than one electrode, a relative-firing rate is easily extracted from the single electrode recording. Also, MUA is more stable over time than single-unit spikes, and it is more informative than single-unit spikes or the LFP.[46] After extracting the MUA, the signal is normalised and its log value is calculate. This way, it is possible to obtain a measure of relative spiking range robust to large fluctuation due to nearby spikes. This measure displays a bimodal behaviour similar to intracellular recordings and HGR, so the same method can be used to extract the Up-and-Down states.

4.3 Analysis of states across different recordings

Even though the previous methods provide a lot of information concerning each recording they are applied to, we want to be able to compare different recordings. For that matter, we need a measure that can be used to assess

the quality of each method. This measure can then be used to compare different recordings and different methods. Also, we are interested in extracting temporal information from the wave propagation. For these problems, we use two different measures.

Coincidence Index - There are several methods that can be used to produce the Up-and-Down state information, and they produce different results. Due to that, it is convenient to have a measure of comparison. One way to tackle this problem is to use the Coincidence Index (CoIn).[30]

Given two or more sequences of Up-and-Down states, it is possible to see how much their states overlap with one another, and give a score based on that.

Let us first consider the CoIn regarding the Up-state. A sequence of states for each recording can be defined by a binary string of 0's and 1's, where 0 represents the Down-state and 1 the Up-state. This way, for a given sequence, X_i, the total length of its Up-states is given by:
$L_X = \sum(X) = \sum_{j=1}^{dim(X_i)} x_j$. Given the sequences of states X,Y,Z, we can define the CoIn as:

$$CoIn_{Up_{X,Y,Z}} = Intersection(X, Y, Z)/Mean(LX, LY, LZ) \tag{4.1}$$

Which is easily generalised to more sequences.

Notice, however, that the CoIn for the Up-state is not the same for the Down-state. For example, for the sequences $[100011], [011000]$, the $CoIn_{Up}$ is 0, whereas the $CoIn_{Down}$ is 0.2857 (Figure 4.3).

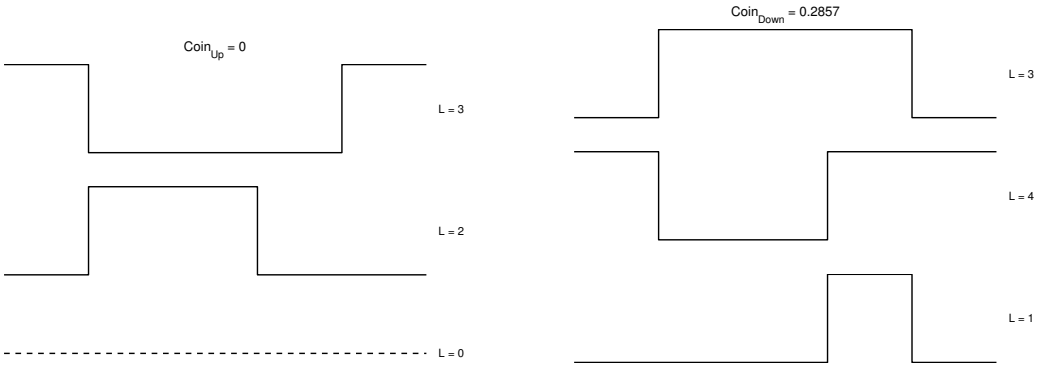

(a) CoIn for the Up-State. (b) CoIn for the Down-State.

Figure 4.3: The Coincidence Index holds different values for the Up-State and the Down-state. For that reason, it is convenient to use an average of both.

For that reason, we use the average Coincidence Index, $CoIn_m$.

$$CoIn_m = \frac{CoIn_{Up} + CoIn_{Down}}{2} \tag{4.2}$$

This way the $CoIn_m$ is a measure of Coincidence between the classification of both states, and from this point onward, the term Coincidence Index will be used to refer to the average of both the Up-and-Down state Coincidence Index. It has the value 1 if all sequences are a perfect match (identical), 0 if they completely mismatch (the inverted version of the signal). Low scores of coincidence can be due to phase differences, differences in states or bad state classification. On the other hand, values above 0.5 mean that there is coincidence between the state classification.

Estimate of lag - Considering that the sleep slow oscillation is a travelling wave across different parts of the brain[41][25], another interesting parameter to estimate is the average delay between them. This delay will show, on average, how long it takes for the wave to be present in different parts of the brain, or how much a brain region lags behind the other. A way to estimate this lag is using cross-correlation.
Correlation is defined in Ifeachor and Jervis, 2002[13], as a measure of the degree of interdependence of one signal to another, or how similar these two signals are. One way to see it is as the sum of the multiplication of one signal by the other. If both are similar, their product will be positive; if they are random, their sum will tend to zero, and a negative sum would mean that one increases as the other decreases. This concept then needs to be normalised by the number of samples, and take into account that signals might be equal, but shifted in time. To do that we divide by the total number of sample, and compute the multiplication of the first signal X_1, by a shifted version of the second one, $X_2(-j)$.

$$r_{12}(j) = \frac{1}{N} \sum_{n=0}^{N-1} x_1(n) x_2(n+j) \tag{4.3}$$

For two different signals, the previous equation is the cross-correlation at time point j. Cross-correlation can also be referred to as sliding dot product or sliding inner-product, and the previous operation be represented by the $\star$ product.
It can be used to determine the delay between two signals, as the signals will present a higher correlation when they are more similar. Since the signals have been shifted in time, we can look into what delay maximizes the cross-correlation (figure 4.4). We will consider this value as the lag between both parts of the brain.

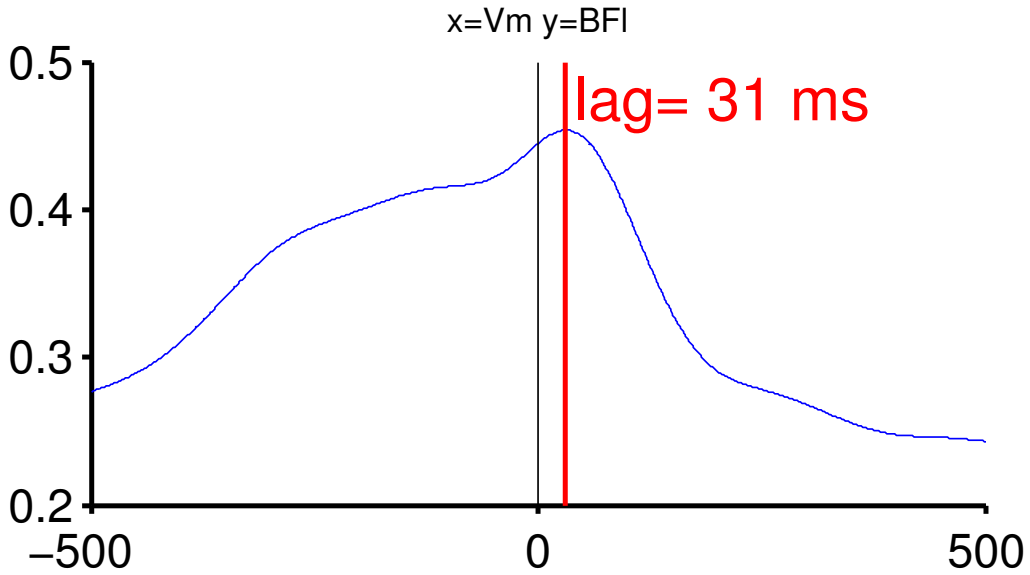

Figure 4.4: Lag between cortical cell and ipsilateral barrel field. For this recording, the Up-states occurs on average 31ms later in the ipsilateral barrel field than in the measured cortical cell.

In the previous example, the lag between Vm and BFl means that on this particular recording, the Up-and-Down states occurred on average 31ms before on the extracellular recording (BFl), then on the whole-cell recording (Vm). A positive lag, means that the first variable is delayed, whereas a negative lag means the second variable is delayed. Notice, however, that in this context a delay depends not only on the states starting earlier or later, but also on their duration. The method is based on cross-correlation, and not on state transition.
Given the sequences of states X_1 and X_2, we can formally define the lag as:

$$\tau = arg_t max(X_1 \star X_2(t)) \tag{4.4}$$

For the analysis of lag, we work with average results across several recordings, since most waves are generated in prefrontal-orbitofrontal regions and propagate in an anteroposterior direction. [25]

Chapter 5

Implementation challenges - The 101

The implementation of the previously described methods does not come without its hurdles. It is during the implementation process that one is faced with common problems, such has dealing with noise, filtering data or finding outliers. In this section we tackle these problems in the intracellular recordings, the extracellular, and problems common to both types of recordings.

5.1 Intracellular recordings

As mentioned before, the intracellular recordings present a golden standard for Up-and-Down state classification that has been used since its first quantification. Even though histogram-based methods are easy to implement, they do present some limitations. One such limitation is the need of a stable recording during the time interval used to calculate the histogram.[30] One typical perturbation to electrophysiological recordings are movement artefacts, such as respiratory movements, heartbeat or muscle movement. These were taken into account during experiment design, and as such the experimental method minimizes them by having the animal under anaesthesia, and by performing tracheotomy. Other forms of disturbance are membrane potential drift or changes in the electrode seal. These will cause the baseline potential to wander, and therefore blur the standard bimodal distribution of up and down states, making it hard to separate the two states based simply on threshold.

Changes in Baseline wander - Intracellular recordings are obtained through the method of patch clamping, and as part of the process it is necessary to

obtain a giga seal and then successfully patch the cell membrane. Once this is achieved, it is possible to measure the membrane potential. The electrical activity of the soma is characterised by an hyperpolarised membrane potential during the Down-state. If the Gigaseal was not done properly, there is no proper isolation of the currents measured across the membrane, and the cell potential will start to fluctuate, jeopardising the recording.
One way to counteract cell depolarisation is to inject current into the cell. This will patch the voltage at a lower value, which can allow a recovery of the Gigaseal. In such case, it is once again possible to read the cell electrical activity, but this process will introduce a baseline wander artefact into the data.(Figure 5.1)

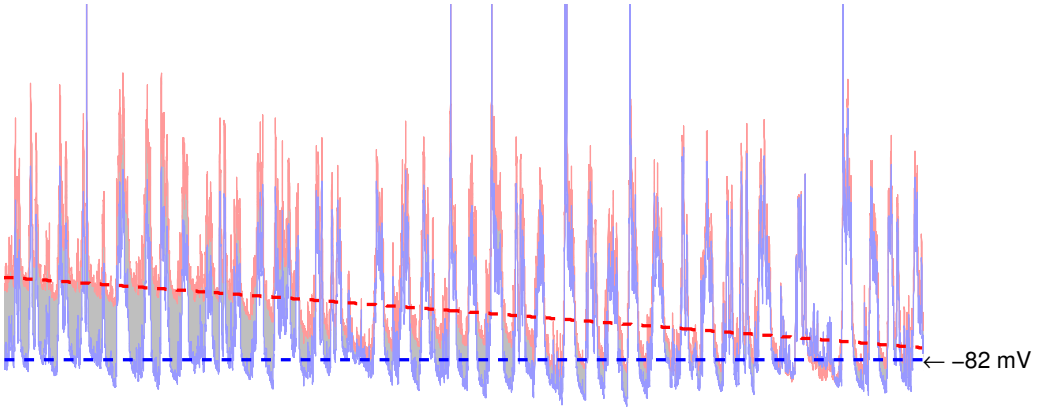

Figure 5.1: Signal before and after removal of baseline wander. In red is the recording before processing and in blue after processing. The data was fitted using exponential curves, represented by the thick dashed line. The area in grey represents the difference between the two signals.

Baseline wander is a distortion of the acquired signal, that leads to a slow variation of the isoelectric line. In order to remove it, we used a linear filtering, time-invariant approach. [45]
This effect was filtered using a Forward-Backward IIR filtering. This was based on a 2^{nd} order Butterworth IIR digital filter, with a cut-off frequency of 0.5 Hz. This type of filter has a low order and is suitable for processing offline data. It can also be extended to a time-variant approach and to online data, by the inclusion of a delay.
This filtering will also remove any DC offset, so the baseline must be restored to its previous value. Since the previous baseline had wander, adding a DC offset equal to the mean of the signal would not be meaningful. For that

reason, the downstate potential is used instead. The downstate potential is the lowest potential where the recording remained, therefore it is possible to identify it as the highest peak with the lowest potential on the histogram (figure 5.2).

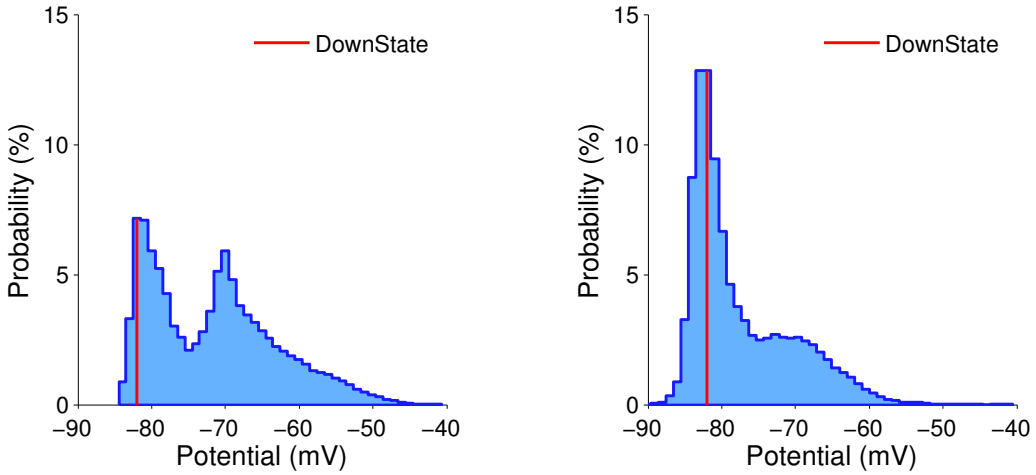

(a) Histogram before baseline wander removal.

(b) Histogram after baseline wander removal.

Figure 5.2: Detection of Downstate potential in a recording with baseline wander. a) Before baseline wander correction, the recording displays two low potential peaks and it is possible to identify the downstate as the most common, lower value of the recording. This correspondes to the lowest peak in the histogram. b) After baseline wander correction there is only one low potential peak, that corresponds to the down-state.

Notice however, that in the few recordings where injection of current was needed to prevent loss of the Gigaseal, the cell is patched at a lower potential level, and therefore the up and downstate potentials might not be representative of the actual cell state potentials.
To further understand the impact of baseline wander removal on electrophysiological recordings, we applied the same processing to recordings where no baseline wander was present. As can be seen in figure 5.3, baseline wander removal improves detection of the downstate, while maintaining the signal properties. Visual inspection of the data and posterior analysis of extracted parameters support this claim.

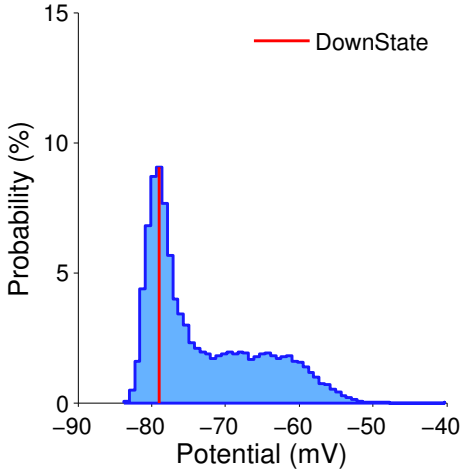

(a) Histogram before baseline wander removal.

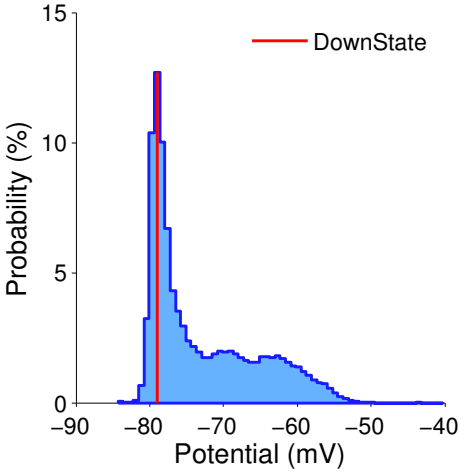

(b) Histogram after baseline wander removal.

Figure 5.3: Detection of Downstate potential in a recording without baseline wander.a) Before baseline wander correction, there is a clear downstate. b) After baseline wander correction the detection of the downstate is improved and there is little to no corruption of the other components of the signal.

5.2 Extracellular recordings

The methods used for extraction of the Up-and-Down state were automated an applied to all recordings. After processing the recordings from dorsolateral MSNs and both barrel field cortex, these showed an interesting trend. When comparing the coincidence between the states in the different recordings using the MUA method, it seemed that the contra barrel field, in respect to the striatum, had always a high coincidence with the intracellular striatal recording, but the Ipsi barrel field, in respect to the striatum, obeyed a bimodal distribution. This distribution (see Figure 5.4) showed that on some experiments there was a high coincidence (similar to the right barrel field), but on others its coincidence index dropped to 0.4. Similar results were obtained for the Wavelet method.

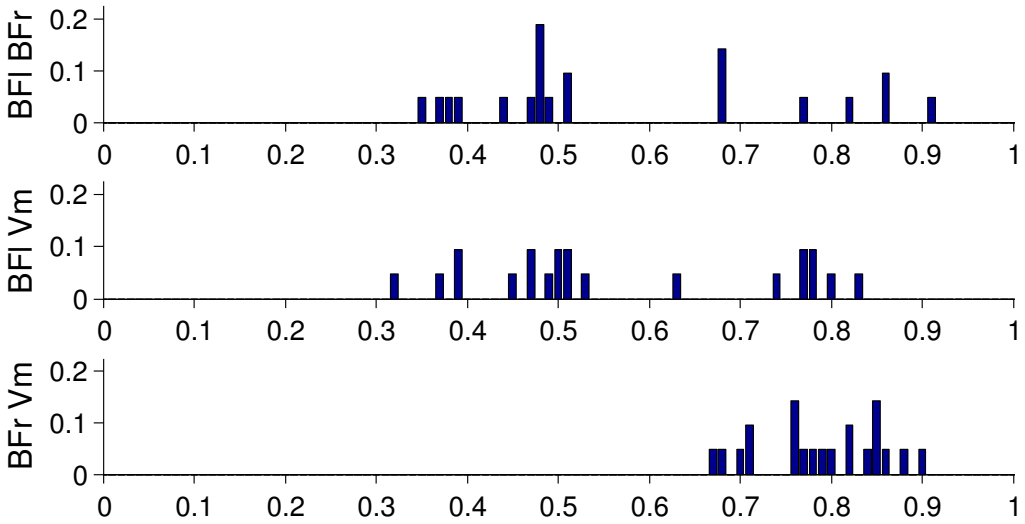

Figure 5.4: Two types of Coincidence Index values. The distribution of the CoIn values shows a bimodal distribution.

The difference between these two types of recordings could either be due to a noise artefact, or to an intrinsic biological difference. In order to discover the source of such effect, we looked into the signal and respective state classification. As can be seen in figure 5.5 there is a misclassification of the Up-and-Down states.

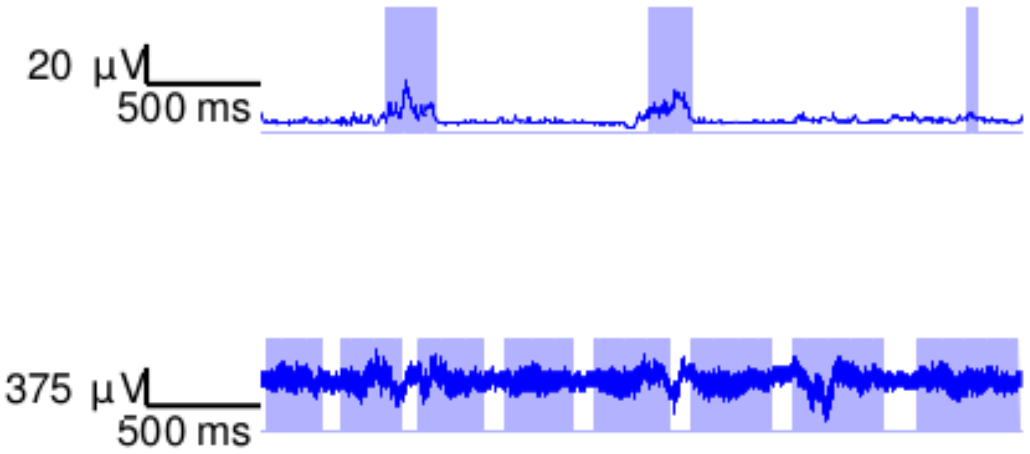

Figure 5.5: Improper detection of Up-and-Down state. The automated Up-and-Down state classification did not work properly in some recordings.

A closer analysis of the spectral content of a recording where the coinci-

dence index was lower revealed that the recording for the left barrel field was contaminated with electric hum of 50Hz and respective harmonics (Figure 5.6).

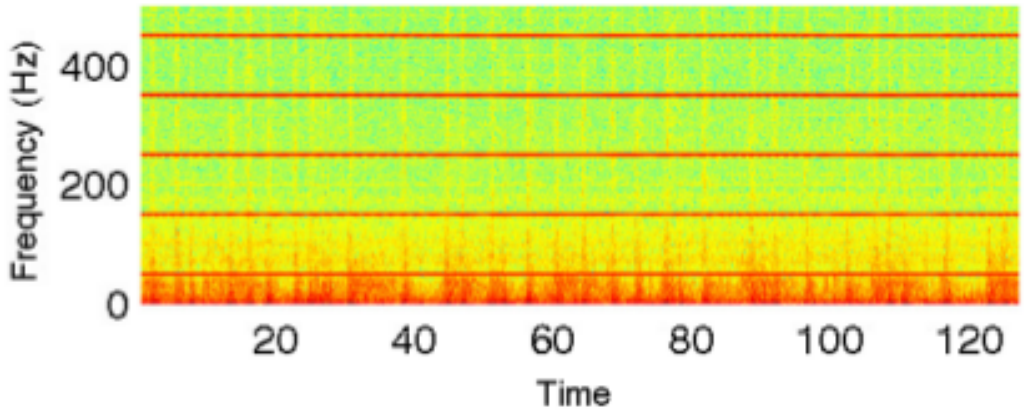

Figure 5.6: Presence of electric hum. The spectrogram of the signal shows a high power in the 50 Hz frequency, and its harmonics.

Because of this particular source of noise, the signal was filtered with an IIR comb filter, with 20 notches and a notch bandwidth of 3 Hz referenced to the -4dB level. The filter has a shelving filter order of 4 and a sampling frequency of 1000 Hz. Because the notches are equidistantly spaced in the interval [-500, 500] Hz, they occur at multiples of 50 Hz.
After digitally filtering the signal, the Up-and-Down state qualification improved substantially. (figure 5.7)

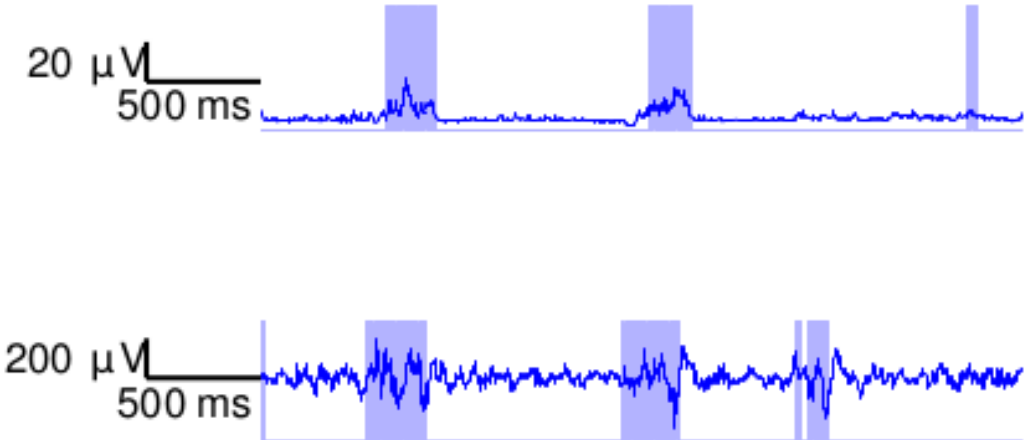

Figure 5.7: Detection of Up-and-Down state after filtering of main hum. After filtering, the state qualification improved has can be visually inspected here.

5.3 General problems

A part from the specific problems found with intracellular and extracellular recordings, other sources of noise had to be address that are common to both types of recording.

Downsampling - All recordings were down sampled to 1000Hz, in order to reduce file size and ease the computation. By down-sampling the signal to 1000 Hz, we still maintain all frequency properties of interest, since we respect the Nyquist-Shannon sampling theorem.

Removal of Artefacts - In some recordings, there are noise artefacts. These can have varied sources, for example, in figure 5.8 you can see a sudden variation of potential. This phenomena was seen across all simultaneous recordings. It was most likely due to a mechanical vibration, that displaced the electrodes.

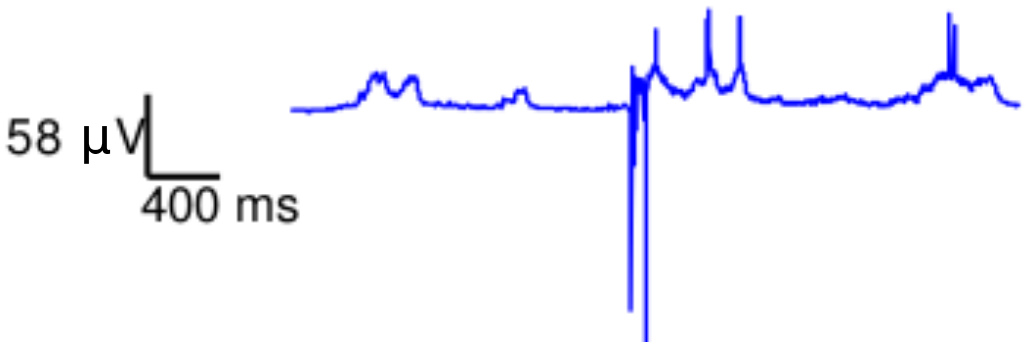

Figure 5.8: Noise artefact. Notice how there is a sudden variation of potential in the middle or the recording.

This kind of sudden variation can be addressed by discarding a small percentile of the data. For my processing, I discarded the top and bottom 0.25 percentile. This was done by removing these values and interpolating the remaining data.

This approach also reduces variation of potential due to spikes, which does not harm our analysis. In fact, it enhances Gaussian fitting, by removal of extreme values.

How to threshold: Mixture models - Using histogram-based methods to discriminate the Up-and-Down state is a well established technique, but the principles used for thresholding can vary. Even though a threshold value can be automatically determined, for example, through the usage of k-means

with 3 clusters[30], it is usual for it to be user defined, based on expert assessment.[42]
Here, due to the volume of data and desire for automation, we opted for using an automated method. The threshold is found, using a Gaussian mixture model with two components to generate a classifier. This is equivalent to fitting two Gaussians to the data and finding their intersection (see figure 5.9). [4]Assuming that each state is normally distributed, the intersection is a suitable candidate for threshold, as it represents the equiprobable point for both states.

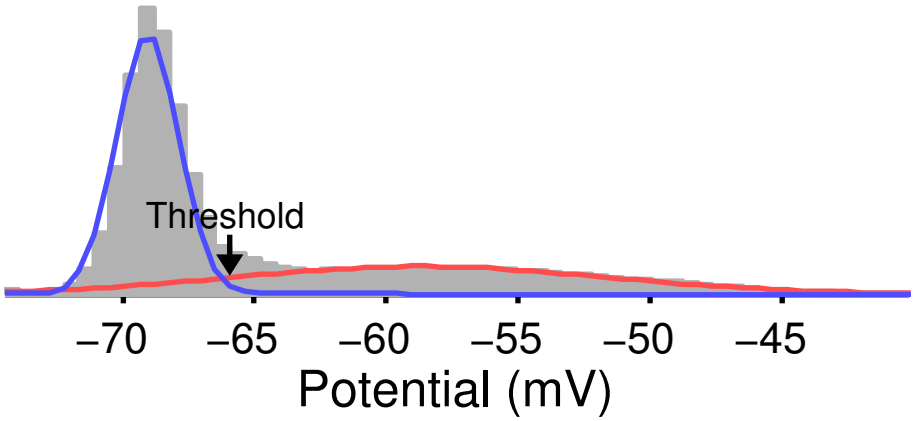

Figure 5.9: Detection of Threshold using Gaussian Mixture model. The red and blue line represent each of the Gaussian distributions fitted to the data. Their interception corresponds to the point that is equally probable to be an Up or Down state, and as such, a suitable candidate for the threshold value.

Once the threshold has been found, it can be used to generate a classifier. This classifier separates the data into two clusters, for which the mean should be different. We perform a verification step, to access if the Up-state mean is higher than the Down-state.
For the extracellular characterisation of the Up-and-Down states, two of the three methods used to process the signal extract properties that also obey a bimodal distribution. For these, we also apply Mixture models to determine the Threshold used for separation of states.
Removal of short Up-and-Down states - Since the Up-and-Down state

detection methods rely on thresholding the cell potential, they are prone to classify very short fragments of the signal as either state. These interruptions of the states, due to occasional noise-driven crossings of the level, do not represent actual states, and should be removed. This was accomplished by locating the two nearest turning points and checking if the width between them was smaller than 40 ms. If so, this time interval should be inverted. This way short Up-states were turned into Down-states, and vice-versa; making longer continuous states.

Precautions filtering - Since all processing was done offline, most of the solutions implemented are Backward-Forward IIR filters, as they allow for lower order filters, and do not alter the phase of the signal. For a formal deduction of the Backward-Forward filter properties see [45].

Another problem faced while filtering was filter transients. When digitally filtering a signal, the filter will output a transient component that requires some time to settle, before the output assumes the expected values. For this reason, before filtering, the signal needs to be padded. Padding consists in adding samples to the signal. A common approach is to add zeros, but these do not conserve the properties of the signal. For that reason, we opted for mirroring the signal, in both the beginning and ending, as it reduces the transient between the 0-padded area and the actual signal.

Statistical analysis - Statistical analysis was carried using the Matlab® one-way ANOVA and N-way ANOVA. Analysis was then carried using the function multcompare. In Matlab® , the function multcompare works by estimating comparison intervals based on a user defined *alpha level*, therefore, when significance was found, it was tested for the values of 0.05, 0.01 and 0.001.

During the analysis of recordings with whole-cell patch clamp of the cortex, the statistical analysis was adapted to take into account the small dataset and the fact that the results of the different methods are dependent on the cells analysed.

Chapter 6

Data Analysis - Catching the Wave

After implementing the different methods and correcting the main sources of noise, it is time to extract and analyse the slow oscillation. It is by capturing this wave, that it can be determined which extraction method is better, and then study the propagation of the wave into the striatum.

6.1 Comparison of different methods

Unlike the intracellular recordings, the extracellular recordings do not obey a bimodal distribution, and therefore the Up-and-Down states must be recovered using other signal properties. Different properties allow the development of different methods, and so we implemented three different methods. These methods hold different results and as such, a comparison of performance is necessary to establish which is more suited for the analysis. One way to compare these results is the Coincidence Index [30]. As stated before, the coincidence index is a measure of similarity between the Up and Down states in different recordings. Considering that intracellular recordings provide a golden standard for the definition of Up-and-Down states, by comparing it to each method, it is possible to assess the quality of the different methods. Since extracellular activity of the cortex is related to its individual cells response, there is coincidence between the states in whole-cell patch clamp of cortical cells and the states of extracellular recordings of the cortex[30].
For this analysis, n=6 cells were used, where we recorded both whole-cell patch clamp measures of cortical cells (Vm), and extracellular recording of the ipsilateral barrel field (BFl). Of those, n=2 contained the extracellular recording of the contralateral barrel field (BFr); and n=2 contained the extracellular recording of the primary visual cortex (V1). Data regarding V1

is not presented here, due to lack of significance.
All recordings had approximately 120s, for which Up-and-Down states were extracted. The CoIn and delay were calculated for each combination of extracted states. Data regarding lag is not presented, due to lack of significance.
We performed this analysis to three different methods, to identify which method fares better in detecting coincidence between the intracellular and extracellular recordings of the cortex. We also verified another biological feature, the methods should detect is a high coincidence between opposing barrel fields.

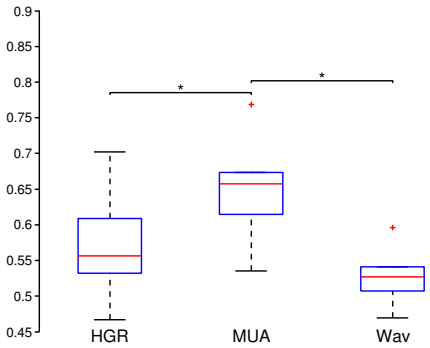

(a) MUA best captures the Up and Down state similarities.

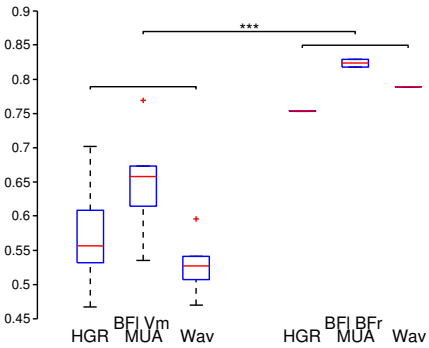

(b) Barrel fields of both hemispheres are closely related.

Figure 6.1: All three methods capture the coincidence between different areas of the cortex and the intracellular recordings. a)MUA's coincidence index is higher on average for the connectivity between the ipsilateral barrel field and its cells. b)All three methods capture that the coincidence index between the ipsilateral and contralateral barrel field is significantly higher than that of the ipsilateral barrel field and its individual neurons.

As can be seen in figure 6.1(a), the MUA method outperforms both the HGR and Wavelet decomposition in detection of Up-and-Down states. The difference between it and competing methods is statistically significant ($p < 0.05$). This comparison was performed using repeated measures ANOVA. Repeated measures ANOVA was selected, as opposed to a standard One-way ANOVA, since we are comparing the performance of different methods, whose output is extracted from the same measurements. Therefore, these outputs are not independent from one another. Another concern was the small sample size, so a Shapiro-Wilk parametric hypothesis test of composite normality was performed[43]. The null hypothesis (normal data) was not rejected.

Regarding coincidence between opposing barrel fields, the results can be seen in 6.1(b). All methods capture a statistical difference ($p < 0.001$) between coincidence of both barrel fields and coincidence of intracellular recording and ipsilateral barrel field. This comparison was done using 2-Way ANOVA. For the following analysis, only the data concerning the MUA method is presented.

6.2 Propagation of Up-and-Down state to the Striatum

It has been shown that the Slow Oscillation propagates throughout the cortex and from the cortex to the striatum. In fact the striatal Up-state is sustained through excitation from the cortex and thalamus.[15] Stimulation of cortical regions can induce a transition to Up-state in cortex and the striatum and similarly, an inhibition of the cortex can lead to an hyperpolarised state.[16] A pertinent question that arises is, what areas of the cortex influence the striatum, and do different parts of the striatum respond differently to different cortical inputs.

Dorsolateral medium spiny neurons - The majority of neurons present in the striatum are medium spiny neurons (MSNs). These are distributed throughout the striatum, and different parts of the striatum, can show different connectivity. We recorded a total of n=46 dorsolateral striatal (DLS) cells using whole-cell patch clamp, with respective extracellular recordings of ipsilateral cortical barrel field (n=46), contralateral cortical barrel field (n=21), visual cortex area V1 (n=20) and motor area M1 (n=5).

If we take into account the relationships between the whole-cell recordings of dorsolateral striatal cells and the different parts of the cortex, it is possible to see that dorsolateral MSNs activity is more closely related to barrel field (S1), than to the visual (V1) and motor (M1) cortex. (See figure 6.2)

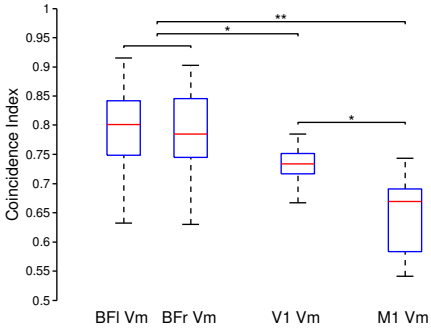

(a) Connectivity between the Up-and-Down state in the cortex and the dorsolateral striatum.

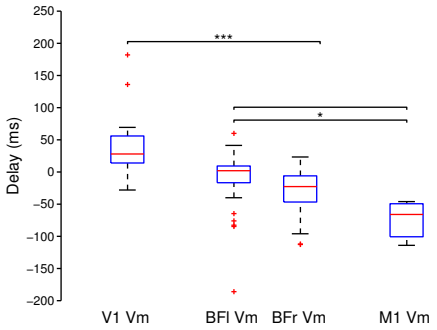

(b) Delay in the propagation of the Up-and-Down state to the dorsolateral striatum.

Figure 6.2: The dorsolateral medium spiny neurons Up-and-Down state resembles most closely the barrel field than other parts of the cortex. (a) They coincide more closely to the barrel field and (b) their delay between the states is smaller.

As seen in 6.2(a), there is more coincidence between the dorsolateral MSNs and the activity in both barrel fields, than to the other areas ($p - value < 0.01$). Even though they show preference for information conveyed from the barrel field, they still receive inputs from both the Visual and motor cortex, where the visual information is of higher importance than the motor ($p - value < 0.05$). Considering the high connectivity between barrel fields and DSL, it was expected that the delay between states would be close to zero. This is the case for the ipsilateral field ($\tau_{(Vm,BFl)} = 9.24ms$), but not for the contralateral ($\tau_{(Vm,BFr)} = 30.1ms$). The motor cortex state precedes the ipsilateral barrel field ($p - value < 0.05$). Notice that, unlike sensory and motor cortex, the visual cortex state does not precede the MSNs. ($p - value < 0.001$).

Wave on the cortex - In order to better understand the propagation of information, it is important to analyse the slow wave oscillation and its propagation within the cortex.

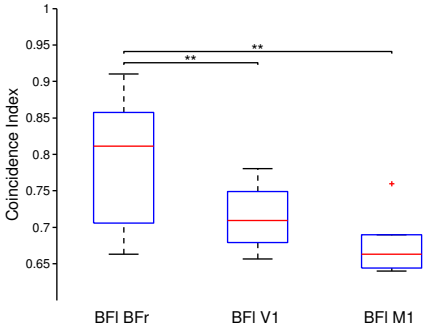

(a) Connectivity between the Up-and-Down state in the cortex.

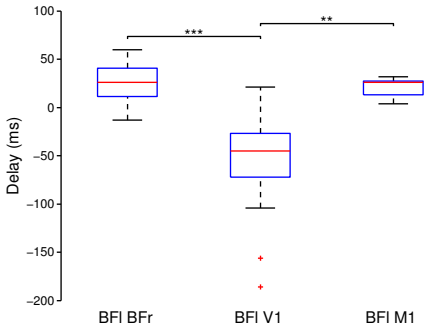

(b) Delay in the propagation of the Up-and-Down state in the cortex.

Figure 6.3: Propagation of the Sleep Slow oscillation in the cortex, in relationship to the ipsilateral barrel field.

The states are more coincident between barrel fields, than they are between the ipsilateral barrel field and V1 or M1 ($p-value < 0.01$) (see Figure 6.3(a)). This relationship is similar to the one found between the DLS and the cortex, supporting the idea that dorsolateral MSNs are more connected to the barrel field than to other parts of the cortex. More so, if we look at the delay between the ipsilateral barrel field and the contralateral one, this has a mean of $\tau_{(BFl,BFr)} = 25.6ms$. Looking now at the delay between the contra barrel field and DLS, we have:

$$\tau_{(Vm,BFr)} \approx \tau_{(BFl,BFr)} + \tau_{(Vm,BFl)} = \hat{\tau}_{(Vm,BFr)} \tag{6.1}$$

Taking into consideration the time the wave propagates in cortex, makes the difference between delays of only $4.41ms$. This result is both obtained by comparison of means, and by the mean of differences. A concordance test between $\tau_{(Vm,BFr)}$ and $\hat{\tau}_{(Vm,BFr)}$ is significant ($p - value = 2.7318 \times 10^{12}$), corroborating the idea that the Slow oscillation propagates from the contralateral barrel field to the dorsolateral cells through the intermediary of the ipsilateral barrel field.
The concordance test used was intraclass Correlation Coefficient, using One-Way Random Effects Model.[27]

Dorsomedial medium spiny neurons - For the study of the dorsomedial striatal cells, a total of n=19 recordings were used, with whole-cell patch-clamp recording of a dorsomedial striatal neuron (Vm), extracellular recording of the ipsilateral barrel field(BFl) and primary visual cortex(V1).
If we look at the distribution of CoIn values (figure 6.4(a)), we see that it does not seem to follow a normal distribution. We further looked into how

the data is distributed taking into account the experiment it comes from (we pair the CoIn values based on the experiment) (see figure 6.4(b)).

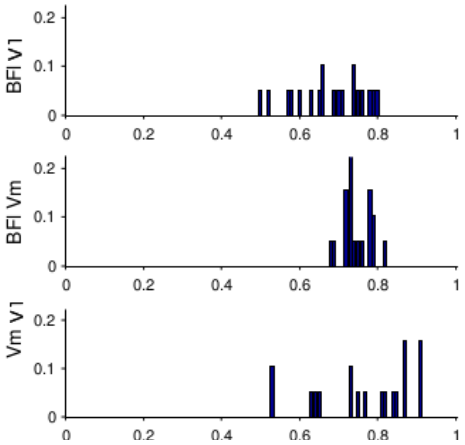

(a) Distribution of coincidence is not normal.

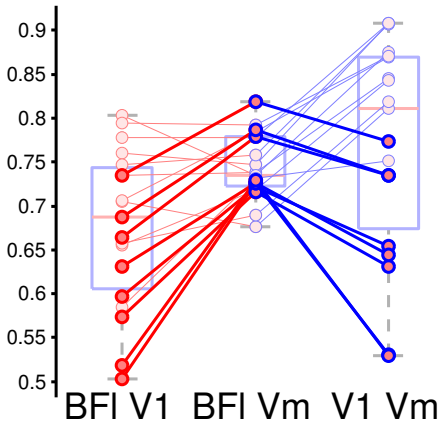

(b) Different connectivity of DMS.

Figure 6.4: Not all DMS show the same behaviour. Distribution of the data(a) is not normal. A closer look at the relationship of the data(b) shows there are two types of DMS, one with $CoIn_{(BFl,Vm)} > CoIn_{(V1,Vm)}$ (darker lines) and other with $CoIn_{(V1,Vm)} > CoIn_{(BFl,Vm)}$ (light colour lines).

The hypothesis that the data is not normal (figure 6.4(a)), was also tested using Shapiro-Wilk normality test. Only the data for $CoIn_{(V1,Vm)}$ could be fitted for $p - value = 0.05$, and they all failed at $p - value = 0.01$. Furthermore, pairing the data based on experiment (figure 6.4(b)), on the principle that data generated by the same cell is not independent, shows that there are two distinct types of dorsomedial striatal neurons. Those that have higher connectivity with the ipsilateral barrel field, and those that have higher connectivity with the primary visual field. We separated the data into two distinct datasets, based on the principle:

$$CoIn_{(BFl,Vm)} > CoIn_{(V1,Vm)} \tag{6.2}$$

This shows that 36.8% of the cells are more connected to the ipsilateral field (n = 7) and 63.2% are more connected to the visual field (n=11). Previous studies in this lab showed similar results, recurring to whisker and visual stimulation to study neuronal response. [35]
Analysis of the two separate datasets reveals different coincidence between states for each group. (see figure 6.5)

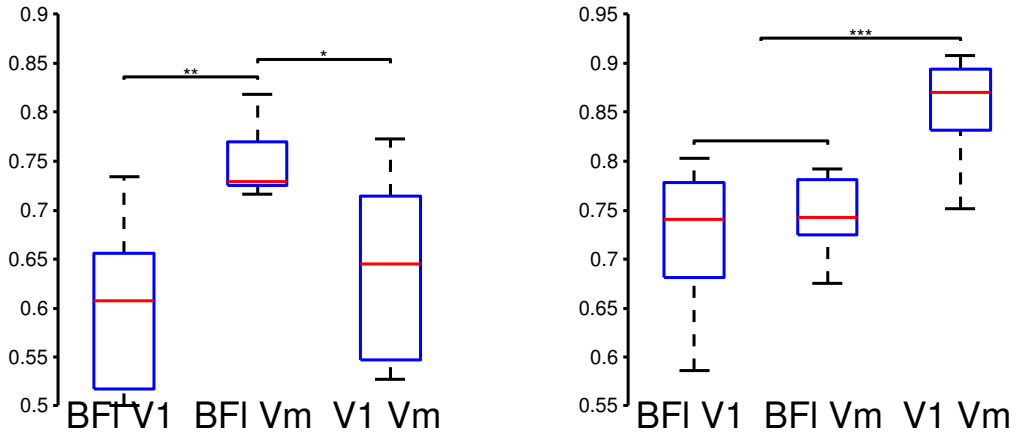

(a) DMS that responde more to ipsilateral barrel field

(b) DMS that responde more to primary visual cortex

Figure 6.5: Two different type of connections in DMS. The DMS on (a) coincide more with the ipsilateral field than with the primary visual cortex. On the other hand, DMS on (b) are more coincident with the primary visual cortex.

For the cells where the coincidence was higher with the barrel field, there is a statistically significant difference between $CoIn_{(BFl,Vm)}$ and $CoIn_{(V1,Vm)}$ ($p-value < 0.05$); and between $CoIn_{(BFl,Vm)}$ and the travelling wave in the cortex $CoIn_{(BFl,V1)}$ ($p - value < 0.05$) (see figure 6.5(a)). Information regarding the delay in the wave corroborates this point (see equation 6.3 and table 6.1).
Concerning the cells that are more coincident with the visual cortex, there is a statistically significant difference between $CoIn_{(V1,Vm)}$ and both $CoIn_{(BFl,Vm)}$ and the traveling wave $CoIn_{(BFl,V1)}$ ($p - value < 0.001$). This means that the coincidence between these DMS and V1 is more relevant than the ipsilateral barrel field, and the fact that the coincidence to the barrel field and to the travelling wave is very similar, might represent that these DMS are also connected to BFl.
Taking the information regarding the delays, we verify the following lag relationship for both types of neurons (see table 6.1):

$$\tau_{(V1,Vm)} \approx \tau_{(BFl,Vm)} - \tau_{(BFl,V1)} = \hat{\tau}_{(V1,Vm)} \tag{6.3}$$

Furthermore, by looking at the average delays, not only do we verify this relationship, but also that for the DMS that respond to the barrel field, their change of state precedes the arrival of the wave to the visual cortex, meaning that the Up-and-Down state is mainly driven by the barrel field activity. For the DMS that respond to V1, the delay is minimum to the visual cortex,

showing that the transition in the visual cortex could be what triggers the transition in the DMS cell. Also, the fact that the delay between the visual cortex and the barrel field is almost the same as between the DMS cell and the barrel field, supports this idea that the striatal cell will only transition once the wave arrives to the visual field.

Dominant connection	$\tau_{(V1,Vm)}$	$\tau_{(BFL,V1)}$	$\tau_{(BFL,Vm)}$	$\hat{\tau}_{(V1,Vm)}$	$p - value$
Barrel Field	55.4286	-76.4286	-24.1429	52.2857	2.0863×10^{-04}
V1	-0.3333	-56.5833	-62.3333	-5.7500	3.8790×10^{-06}

Table 6.1: Temporal relationship for dorsomedial striatal neurons. This data supports the relationship expressed in equation 6.3.

The p-values shown in table 6.1 are the concordance test between $\tau_{(V1,Vm)}$ and $\hat{\tau}_{(V1,Vm)}$. and support the relationship between the propagation of the wave in the cortex, and to the dorsomedial striatum (equation 6.3).
The concordance test used was intraclass Correlation Coefficient, using One-Way Random Effects Model.

Chapter 7

Discussion - Deliberating the scores

In this study we compared the performance between different methods of extraction of the Up-and-Down state from extracellular recordings. Our findings confirm the idea that methods based on high-frequency outperform those based on wavelet decomposition. More so, the method based in the high-frequency range ($> 200Hz$), which is an approximation of the spiking activity, outperforms the method based on High-Gamma frequencies ($20 - 100Hz$). One important note on our analysis is that unlike in the original paper from Mukovski (2007)[30], we did not pre-select our recordings. In their study they defined a formal criteria based on the ratio between power below and above 4 Hz, for which only recordings with a ratio higher than 3.5 are considered, guarantying a deep NREM sleep state. Our recordings, on the other hand, do show bimodality, but were not picked based on any formal criteria. In our study, the animal was under the effect of anaesthesia, which induced slow oscillations. These might differ from deep NREM sleep. Another source of biological variability is the animal model itself. Whereas the original study was done in cats, our study is conducted in mice. Due to these variabilities the frequency relationship on which the method is based might not hold. In fact, an analysis to the frequency components of our cortical recordings show that the power ratio for the Up and Down state was consistently higher for high-frequencies ($> 200Hz$, data not show here). For this reason, we believe that our results using the HGR method for classification of the Up-and-Down state did not held similar results to the original paper. Nonetheless, the MUA method did present high indexes of coincidence, outperforming HGR and proving to be a reliable and robust method. In regard to the comparison of the different methods, our sample size was small (n=6), and even though the statistical analysis used was adequate, techniques of re-sampling (e.g. bootstrap) and/or cross-validation (k-fold validation) could have been used.

The measure used to compare recordings was the Coincidence Index, but this value is affected by both displacements in time and differences in the actual states. For example, a sequence with a phase shift of 45° will have a CoIn of 0.5, which is the same for a sequence with half the period. For this reason, we propose using cross-correlation to extract independent information about state coincidence and phase delay for similar studies. Notice, however, that cross-correlation for calculation of phase delay is only suited for signals with sufficient correlation. Other options could involve CoIn corrected for lag, or quantities of information, such as mutual information.

Once we established the MUA as our method of extraction of the slow oscillation, we could study how the wave propagated in the cortex and how different cells in the striatum responded to it. Our results support a specialisation of the dorsolateral striatum to signals coming from the primary sensory cortex, whereas the dorsomedial striatum responds both to somatosensory and visual information. Some cells relate more to sensory information (36.8%), whereas the rest (63.2%) relate more to visual information.

When sufficient data is available, it is possible to study how the slow oscillation travels in the cortex. By comparing time delays between cortex and striatum it is possible to infer time dependencies, which are correlated to connectivity. Considering the dorsolateral striatal cells, there is a time relationship that shows that information from the contra barrel field is propagated to the ipsilateral barrel field, which then conveys it to the striatal cells. This is expressed in equation 6.1. This is in line with previous findings from our group [35].

For the dorsomedial striatal cells we extracted a time relationship (equation 6.3), that applies to both the cells that respond to visual cortex and the cells that respond to the sensory cortex. Notice how for the cells that respond to the primary visual field, the delay $\tau_{(Vm,V1)}$ is very small, but the delay $\tau_{(Vm,BFl)}$ is of the same order as $\tau_{(BFl,V1)}$. This supports the idea that first the slow oscillation travels from the barrel field to V1, where it is relayed to the dorsomedial cell. This is not the case for dorsomedial cells that are more coincident to the barrel field. For those, the delay is higher, which is accordance with the fact that these cells respond to bilateral whisker stimulation, but with a slower and weaker response than the dorsolateral ones.[38].

Interestingly, if we look into the coincidence index between the striatal cells and the barrel field cortex, it is higher than the coincidence between a single cell of the barrel field and its extracellular counterpart. The lower coincidence index between cortical single cell and extracellular recording can be explained by intercell variability[30], whereas the higher values of the striatal cells are due to the integrating properties of the striatum[17] in the selection of motor programs.[10].

This study is also a proof that the slow oscillation can provide functional information and shed light into the connectivity of the brain, even in the absence of stimulation. Functional information is provided by the measure of coincidence, whereas connectivity can be derived from the relationship in delays. Having a wider variety of extracellular recording sites can lead to a better understanding of how the slow oscillatory wave propagates, making it easier to understand when a delay is due to propagation of the wave or due to connectivity.
Concerning the current data, we have extracted several features from the Up-and-Down state across all recordings, such as: duration, frequency, mean membrane potential and cross-correlation. These have not yet been analysed, however cross-correlation seems to be a good candidate to replace the coincidence index as a way to explain connectivity between the cortex and the striatum.
Considering that the results found here are in accordance with the anatomy results and what was found using stimulation, it would be interesting to further compare these results. This way, we could compare the brain in a static, sleep state and its dynamic response to stimuli. Another pertinent question is how does the active stimulation influences the sleep slow oscillations. It has been shown that cortical stimulation produce phase perturbations in MSNs, and that striatal Up states terminate abruptly if its cortical afferents activity is turned off by local electrical stimulation.[16]
If such perturbations influence the Slow-Wave-Sleep, what is the effect of a natural stimulus on its propagation.
Another question that one might ask, is what is the role of the sleep slow oscillation in the striatum, given its importance in memory consolidation.

Bibliography

[1] Allen mouse brain atlas, mouse, p56, saggital. http://atlas.brain-map.org/atlas?atlas=2#atlas=2&plate=100883867&resolution=13.96&x=7767.989501953125&y=4023.687947591146&zoom=-3&z=6.

[2] Adeli, H., Zhou, Z., and Dadmehr, N. Analysis of eeg records in an epileptic patient using wavelet transform. *Journal of neuroscience methods 123*, 1 (2003), 69–87.

[3] Akemann, W., Mutoh, H., Perron, A., Rossier, J., and Knöpfel, T. Imaging brain electric signals with genetically targeted voltage-sensitive fluorescent proteins. *Nature methods 7*, 8 (2010), 643–649.

[4] Barber, D. *Bayesian Reasoning and Machine Learning*. Cambridge University Press, 2012.

[5] Chae, M., Liu, W., Yang, Z., Chen, T., Kim, J., Sivaprakasam, M., and Yuce, M. A 128-channel 6mw wireless neural recording ic with on-the-fly spike sorting and uwb tansmitter. In *Solid-State Circuits Conference, 2008. ISSCC 2008. Digest of Technical Papers. IEEE International* (2008), IEEE, pp. 146–603.

[6] Demiralp, T., et al. Event-related oscillations are 'real brain responses'—wavelet analysis and new strategies. *International Journal of Psychophysiology 39*, 2 (2001), 91–127.

[7] Destexhe, A., and Bedard, C. Local field potential. 10713. revision number 135811.

[8] Diekelmann, S., and Born, J. The memory function of sleep. *Nature Reviews Neuroscience 11*, 2 (2010), 114–126.

[9] Fraser, G. W., Chase, S. M., Whitford, A., and Schwartz, A. B. Control of a brain–computer interface without spike sorting. *Journal of neural engineering 6*, 5 (2009), 055004.

[10] Grillner, S., Hellgren, J., Menard, A., Saitoh, K., and Wikström, M. A. Mechanisms for selection of basic motor programs–roles for the striatum and pallidum. *Trends in neurosciences 28*, 7 (2005), 364–370.

[11] Herrmann, C. S., Grigutsch, M., and Busch, N. A. 11 eec oscillations and wavelet analysis. *Event-related potentials: A methods handbook* (2005), 229.

[12] Huerta-Ocampo, I., Mena-Segovia, J., and Bolam, J. P. Convergence of cortical and thalamic input to direct and indirect pathway medium spiny neurons in the striatum. *Brain Structure and Function* (2013), 1–14.

[13] Ifeachor, E. C., and Jervis, B. W. *Digital signal processing: a practical approach*. Pearson Education, 2002.

[14] Kanda, P. A. M., Trambaiolli, L. R., Lorena, A. C., Fraga, F. J., Basile, L. F. I., Nitrini, R., and Anghinah, R. Clinician's road map to wavelet eeg as an alzheimer's disease biomarker. *Clinical EEG and neuroscience 45*, 2 (2014), 104–112.

[15] Kasanetz, F., Riquelme, L. A., Della-Maggiore, V., O'Donnell, P., and Murer, M. G. Functional integration across a gradient of corticostriatal channels controls up state transitions in the dorsal striatum. *Proceedings of the National Academy of Sciences 105*, 23 (2008), 8124–8129.

[16] Kasanetz, F., Riquelme, L. A., O'Donnell, P., and Murer, M. G. Turning off cortical ensembles stops striatal up states and elicits phase perturbations in cortical and striatal slow oscillations in rat in vivo. *The Journal of physiology 577*, 1 (2006), 97–113.

[17] Kreitzer, A. C., and Malenka, R. C. Striatal plasticity and basal ganglia circuit function. *Neuron 60*, 4 (2008), 543–554.

[18] Lachaux, J.-P., Lutz, A., Rudrauf, D., Cosmelli, D., Le Van Quyen, M., Martinerie, J., and Varela, F. Estimating the time-course of coherence between single-trial brain signals: an

introduction to wavelet coherence. *Neurophysiologie Clinique/Clinical Neurophysiology 32*, 3 (2002), 157–174.

[19] Lee, T. S., Mumford, D., Romero, R., and Lamme, V. A. The role of the primary visual cortex in higher level vision. *Vision research 38*, 15 (1998), 2429–2454.

[20] Lewicki, M. S. A review of methods for spike sorting: the detection and classification of neural action potentials. *Network: Computation in Neural Systems 9*, 4 (1998), R53–R78.

[21] Mallat, S. *A wavelet tour of signal processing: the sparse way*. Academic press, 2008.

[22] Mammone, N., La Foresta, F., and Morabito, F. C. Automatic artifact rejection from multichannel scalp eeg by wavelet ica. *Sensors Journal, IEEE 12*, 3 (2012), 533–542.

[23] Marcia F. Bartusiak, e. a. *A Positron Named Priscilla:Scientific Discovery at the Frontier*. The National Academies Press, 1994.

[24] Massimini, M., and Amzica, F. Extracellular calcium fluctuations and intracellular potentials in the cortex during the slow sleep oscillation. *Journal of Neurophysiology 85*, 3 (2001), 1346–1350.

[25] Massimini, M., Huber, R., Ferrarelli, F., Hill, S., and Tononi, G. The sleep slow oscillation as a traveling wave. *The Journal of Neuroscience 24*, 31 (2004), 6862–6870.

[26] Mattia, M., and Del Giudice, P. Population dynamics of interacting spiking neurons. *Physical Review E 66*, 5 (2002), 051917.

[27] McGraw, K. O., and Wong, S. P. Forming inferences about some intraclass correlation coefficients. *Psychological methods 1*, 1 (1996), 30.

[28] Metherate, R., and Ashe, J. H. Ionic flux contributions to neocortical slow waves and nucleus basalis-mediated activation: whole-cell recordings in vivo. *The Journal of neuroscience 13*, 12 (1993), 5312–5323.

[29] Mölle, M., Yeshenko, O., Marshall, L., Sara, S. J., and Born, J. Hippocampal sharp wave-ripples linked to slow oscillations in rat slow-wave sleep. *Journal of neurophysiology 96*, 1 (2006), 62–70.

[30] Mukovski, M., Chauvette, S., Timofeev, I., and Volgushev, M. Detection of active and silent states in neocortical neurons from the field potential signal during slow-wave sleep. *Cerebral Cortex 17*, 2 (2007), 400–414.

[31] Paxinos, G., and Franklin, K. The mouse brain in stereotaxic coordinates (academic, san diego), 2001.

[32] Pidoux, M., Mahon, S., Deniau, J.-M., and Charpier, S. Integration and propagation of somatosensory responses in the corticostriatal pathway: an intracellular study in vivo. *The Journal of physiology 589*, 2 (2011), 263–281.

[33] Plenz, D., and Kitai, S. T. Up and down states in striatal medium spiny neurons simultaneously recorded with spontaneous activity in fast-spiking interneurons studied in cortex–striatum–substantia nigra organotypic cultures. *The Journal of neuroscience 18*, 1 (1998), 266–283.

[34] Purves, D. *Principles of cognitive neuroscience*. Sinauer Associates Inc, 2008.

[35] R. REIG, G. S. Bilateral and multisensory integration in striatal microcircuits. Program No. 380.11/VV11. 2012 Neuroscience Meeting Planner. New Orleans, LA: Society for Neuroscience, 2012. Online., 2012.

[36] Rechtschaffen, A., and Kales, A. A manual of standardized terminology, techniques and scoring system for sleep stages of human subjects.

[37] Reig, R., Mattia, M., Compte, A., Belmonte, C., and Sanchez-Vives, M. V. Temperature modulation of slow and fast cortical rhythms. *Journal of neurophysiology 103*, 3 (2010), 1253–1261.

[38] Reig, R., and Silberberg, G. Multisensory integration in the mouse striatum. *Neuron* (2014).

[39] Ruiz-Mejias, M., Ciria-Suarez, L., Mattia, M., and Sanchez-Vives, M. V. Slow and fast rhythms generated in the cerebral cortex of the anesthetized mouse. *Journal of neurophysiology 106*, 6 (2011), 2910–2921.

[40] Sanchez-Vives, M. V., Mattia, M., Compte, A., Perez-Zabalza, M., Winograd, M., Descalzo, V. F., and Reig, R.

Inhibitory modulation of cortical up states. *Journal of neurophysiology 104*, 3 (2010), 1314–1324.

[41] Sanchez-Vives, M. V., and McCormick, D. A. Cellular and network mechanisms of rhythmic recurrent activity in neocortex. *Nature neuroscience 3*, 10 (2000), 1027–1034.

[42] Seamari, Y., Narváez, J. A., Vico, F. J., Lobo, D., and Sanchez-Vives, M. V. Robust off-and online separation of intracellularly recorded up and down cortical states. *PloS one 2*, 9 (2007), e888.

[43] Shapiro, S. S., and Wilk, M. B. An analysis of variance test for normality (complete samples). *Biometrika* (1965), 591–611.

[44] Shoham, S., Fellows, M. R., and Normann, R. A. Robust, automatic spike sorting using mixtures of multivariate¡ i¿ t¡/i¿-distributions. *Journal of neuroscience methods 127*, 2 (2003), 111–122.

[45] Sörnmo, L., and Laguna, P. *Bioelectrical signal processing in cardiac and neurological applications*. Academic Press, 2005.

[46] Stark, E., and Abeles, M. Predicting movement from multiunit activity. *The Journal of neuroscience 27*, 31 (2007), 8387–8394.

[47] Steriade, M. Grouping of brain rhythms in corticothalamic systems. *Neuroscience 137*, 4 (2006), 1087–1106.

[48] Steriade, M., Nunez, A., and Amzica, F. A novel slow (¡ 1 hz) oscillation of neocortical neurons in vivo: depolarizing and hyperpolarizing components. *The Journal of Neuroscience 13*, 8 (1993), 3252–3265.

[49] Takekawa, T., Isomura, Y., and Fukai, T. Accurate spike sorting for multi-unit recordings. *European Journal of Neuroscience 31*, 2 (2010), 263–272.

[50] Timofeev, I., Contreras, D., and Steriade, M. Synaptic responsiveness of cortical and thalamic neurones during various phases of slow sleep oscillation in cat. *The Journal of Physiology 494*, Pt 1 (1996), 265–278.

[51] Tootell, R. B., Hadjikhani, N. K., Vanduffel, W., Liu, A. K., Mendola, J. D., Sereno, M. I., and Dale, A. M. Functional analysis of primary visual cortex (v1) in humans. *Proceedings of the National Academy of Sciences 95*, 3 (1998), 811–817.

[52] Torrence, C., and Compo, G. P. A practical guide to wavelet analysis. *Bulletin of the American Meteorological society 79*, 1 (1998), 61–78.

[53] Wilson, C. J., and Kawaguchi, Y. The origins of two-state spontaneous membrane potential fluctuations of neostriatal spiny neurons. *The Journal of neuroscience 16*, 7 (1996), 2397–2410.